# On Prediction of Ground Heave and the Performance of the Isolation-tube Shafts

지반 팽창량 예측과 분리형 현장 타설 말뚝의 거동

Kim, Myung-Hak[*1]
김 명 학
O' Neill, Michael W.[*2]

## 요 지

미합중국 텍사스 주 휴스턴 시 소재의 휴스턴 대학 내에 위치한 미합중국 국립 지반 실험지 (National Geotechnical Experimentation Site at the University of Houston)의 팽창성 점토에 설치된 직경 305mm 1개의 일반 현장타설 말뚝과 3개의 분리형 현장타설 말뚝의 18개월간 의 거동에 관한 실험적 연구를 수행하였다.

지반의 흡수력 변화에 따른 지반 팽창량 예측을 위해 실험 말뚝 주위의 지반에 깊이별로 지반 흡수력 감지 장치를 설치하여 관측한 결과, 지반은 최대 35mm까지 팽창하였고 일반 현장타설 말뚝은 4-5mm, 분리형 현장타설 말뚝은 1-2mm의 수직 변위가 관측되었다.

또한 지반 흡수력, 전압력과 체적 변형률 간의 관계식을 얻기 위해 3축 압축 실험 장치를 변형한 실내 실험을 수행하였으며, 이 결과를 이용하여 최대 지반 팽창량 예측 모델을 만들어 현장 실측치와 비교 검토하였다.

## Abstract

An experimental study, which included four 305mm-diameter test shafts, one reference shaft with standard design and three test shafts with isolation tubes, is described. The soil was also instrumented to track suction changes to permit development of a computational model concerning soil heave and shrinkage that occur during suction changes at the field site.

The test shafts were monitored for a period of about 18 months. Maximum ground movements exceeding 35mm were observed. Movements of only 1 to 2mm were observed in the test shafts with isolation tubes, while movements of 4 to 5mm were observed in the reference shaft.

A simple computing model was developed to predict, based on suction changes, the maximum

*1 정회원, 인제대학교 공과대학 토목공학과 조교수
*2 John and Rebecca Moores Professor: Department of Civil and Environmental Engineering; University of Houston; Houston, Texas 77204-4791, USA

amount of ground heave. Relationship among suction, total stress, and volumetric strain was obtained in the laboratory. This relationship, used as inputs to the predictive model, enabled the computation of the maximum ground heave.

Keywords : Expansive soil, Drilled shaft, Isolation tube, Suction, NGES-UH

## 1. Introduction

Soils with a potential for shrinking and swelling are found throughout the world (Johnson and Snethen, 1978). Such soils are commonly called "expansive soils." These soils are often fissured or shattered, with open or filled joints. Their mass per meabilities, and consequently spatial distributions of water potential, are therefore difficult to be predicted. When the moisture content of such soils increases, the volume of the soil mass increases. This phenomenon is driven by the soil moisture retention potential, termed "soil suction." Soil suction is a negative pore pressure that is directly related to effective stress in the soil framework. Since suction is a component of effective stress, it is an accurate indicator of the volume and strength states of specific soils (Fredlund, 1983; Johnson and Snethen, 1978). Thus, the measurement of suction is an appropriate means of tracking the changes in the volume of expansive soil formations.

Drilled shaft foundations are frequently used to bypass expansive surficial soils that otherwise possess strength and compressibility properties adequate to support shallow foundations (O' Neill and Poormoayed, 1980). However, expansive clays near the surface can exert large shearing stresses on the perimeters of drilled shafts that can produce excessive upward movement and even tensile failures when the shafts support light structures (O' Neill and Poormoayed, 1980). Predicting the volume-change behavior of expansive soils is an important step in geotechnical investigation, foundation selection, and design for areas in which these soils occur (McKeen, 1992).

Expansive soils were recognized in an NSF study as one of the six most damaging natural hazards in the United States (Wiggins, et al., 1978). Wiggins, et al. (1978) indicate that mitigation studies could reduce as much as 35% of the damage associated with expansive soils. Mitigation studies refer to those studies that provide the profession with a better understanding of the problem and the factors that influence it. For example, reduction of volume change can be achieved through preconstruction treatment or adequate structural design of the foundation, both of which rely on an accurate estimate of the potential volume and shear strength changes. This research focuses on the fundamental behavior of drilled shafts in partially saturated soils and ways of mitigating the effects of expansion.

## 2. Description of Site

The experimentation site was the National Geotechnical Experimentation Site at the University of Houston, Texas (NGES-UH). Test site stratigraphy is shown in Fig. 1. The site is flat and vegetated with short, native grass. The soil "loading" was forned exclusively by natural rainfall and atmospheric thermal effects.

Three separate soil strata of concern to this research were identified on the site. The top 2.7m consisted of stiff to very stiff gray and tan clay, which classified as CH in the Unified Soil Classification System. The next 0.8m consisted of a stiff gray and tan very sandy clay with waterbearing sand seams (CL), and the underlying stratum was a stiff to hard red and light gray clay (CH). The last stratum extended to a depth of at least 7m. A little amount of free ground water was encountered at a depth of 2.1m during shaft excavation.

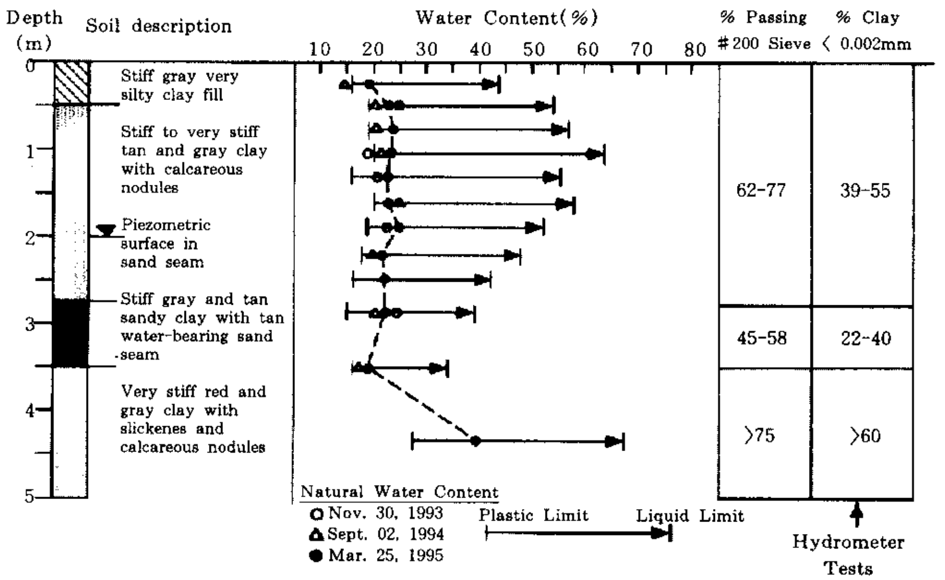


Fig.1 Test Site Stratigraphy

## 3. Laboratory Test

### 3.1 Suction-Total Stress-Volume Change Test

Several researchers have suggested the use of net normal stress $(\sigma - u_a)$ and matric suction $(u_a - u_w)$ as the stress variables for describing volume change behavior (Brackley, 1971; Aitchison and Martin, 1973). The role of $(\sigma - u_a)$ and $(u_a - u_w)$ as stress state variables for an unsaturated soil was demonstrated by Fredlund and Morgenstern (1976). The volume change ratio of an unsaturated soil under general, three-dimensional loading can be written as

$$d\varepsilon_v = C_t \ \Delta \log \ (\sigma - u_a) + C_m \ \Delta \log \ (u_a - u_w) \tag{1}$$

where $\varepsilon_v$ = volumetric strain,

$C_t$ = compression index,

$(\sigma - u_a)$ = net normal stress state variable,

C = suction index in terms of void ratio and matric suction,

$(u_a - u_w)$ = matric suction,

$\sigma$ = mean total normal stress,

$u_w$ = pore water pressure, and

$u_a$ = pore air pressure (usually atmospheric).

For ideal $K_o$ – loading, a total stress increment of $d\sigma_z$ is applied in the vertical direction, while the soil is not permitted to deform laterally (i.e., $d\varepsilon_x = d\varepsilon_y = 0$), so that

$$d\varepsilon_z = C_t \, \Delta\log\,(\sigma_z - u_a) + C_m \, \Delta\log\,(u_a - u_w) \tag{2}$$

where z represents the vertical direction.

Since volumetric strain, $d\varepsilon_v$, is equal to the strain in the vertical direction, $d\varepsilon_z$, for ideal $K_o$ loading conditions, Eq. 1 can be written as follows:

$$d\varepsilon_v = C_t \, \Delta\log\,(\sigma_z - u_a) + C_m \, \Delta\log\,(u_a - u_w) \tag{3}$$

The volumetric strain change, $d\varepsilon_v$, is defined as the volume change in the voids of the soil element dVv divided by the initial volume of element, Vo, or

$$d\varepsilon_v = \frac{dV_v}{V_o} \tag{4}$$

The initial volume, $V_o$, refers to the volume of the soil element at the start of the volume change process. At the end of each increment, the volumetric strain change, $d\varepsilon_v$, can be computed from Eq. 3, and the volumetric change of the soil element, $dV_v$, is obtained from Eq. 4. The summation of the volumetric strain change times the volume of element for each increment of strain gives the final volume change of the soil,

$$V_v = \int_{Z=0}^{Z-Z_C} \int_i V_{oi} d\varepsilon_{vi} dzA, \tag{5}$$

where z is depth, $z_c$ = depth to zero stress change, A is a unit area, and i is a stress increment.

For ideal $K_o$ loading conditions volume change, $V_v$, is equal to the vertical magnitude of heaving, H. Thus, Eq. 5 can be expressed for practical purposes in a numerical solution as

$$H = \sum_{n=1}^{k} \sum_i \Delta\varepsilon_{vi} V_{oi} \Delta z_n, \tag{6}$$

where n is a depth index, $\Delta z$ is a depth increment and k is the number of depth increments used.

Real soils, such as the soils at the NGES-UH, may not expand or contract under ideal $K_o$ conditions. For example, the presence of vertical cracks that develop during shrinkage may result in a lateral component of deformation during the expansion process, which is contrary to the $K_o$ assumption. Laboratory tests can be conducted to determine directly vertical strain in the soil as a function of changes in suction or total vertical pressure, provided the samples are tested with zero lateral strain on the boundaries. If the cracks in the soil are small, they will be contained in test specimens at the same frequency as existing in the ground, so that holding test specimens at zero lateral strain on the boundaries, although not providing $K_o$ conditions at all points within the interior of the specimen, will produce the correct relationship between stress change and vertical strain in the specimen as a whole. If, however, the crack pattern contained within the specimen is not representative of the crack pattern that exists in situ, the experimental relationship will have to be adjusted. Equation 6 should therefore be written as

$$H = \sum_{n=1}^{k} \sum_{i} \xi \Delta\varepsilon_{vi} V_{oi} \Delta z_n, \tag{7}$$

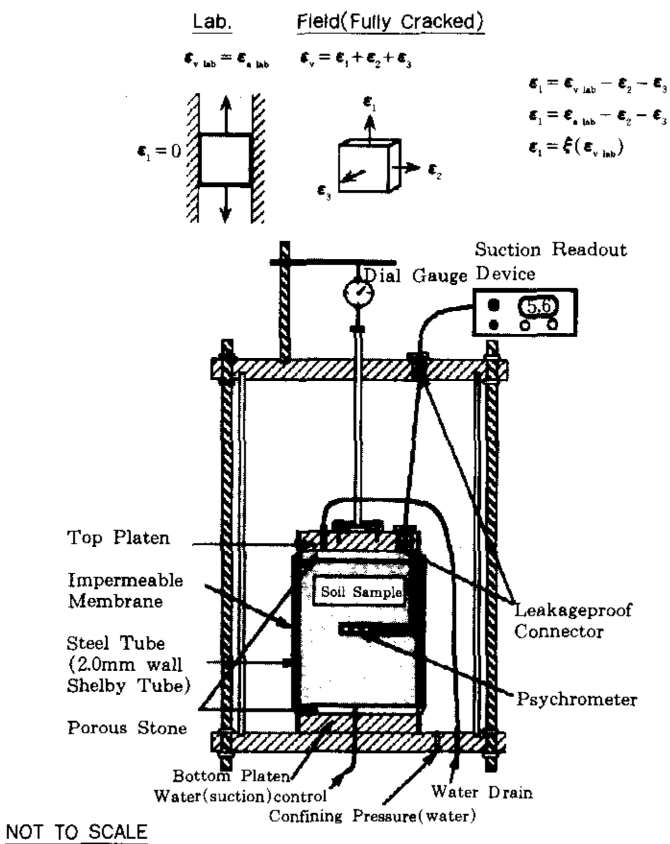


Fig.2 Schematic of Suction-Pressure-Volume Change Test Set-up

in which $\xi$ is an empirical cracking factor that accounts for any deviation from lateral boundary conditions utilized in the laboratory.

### 3.2 Test Arrangement

In order to determine the effects of the stress variables in the volume change strain equation, it is necessary to measure both the net normal stress change and the matric suction change. The conventional triaxial test apparatus was modified for this purpose, as shown in Fig. 2. To measure matric suction change, a suction sensor (psychrometer) was inserted in the middle of the soil sample through a leakageproof connector installed in the top platen. The vertical confining pressure was maintained at the total in situ pressure at the depth of soil sampled. To simulate the $K_o$ condition, an internally lubricated steel tube (2.0mm-wall-thickness-Shelby tube) was slipped over the sample prior to testing to prevent lateral expansion of soil. The volume change was measured at the top of the sample by using the dial gage.

### 3.3 Results of Suction-Pressure-Volume Change Tests

Five different depths of samples were selected (0.45m, 0.7m, 1.1m, 1.6m, and 2.4 m). Before the swelling phase was performed, a cell pressure was applied to each sample. This pressure is applied to the sample only in the vertical direction because of the tube. The mean total confining pressure is then given by

$$\sigma_c = \frac{1+2K_o}{3}\sigma_v, \tag{8}$$

where $\sigma_c$ is mean total confining pressure, and $\sigma_v$ = applied vertical total pressure.

Values of $K_o$ were estimated by using the data taken from O' Neill and Yoon (1995).

Sample data and results of suction-pressure-volume change tests are summarized in Table 1.

The typical result of suction-pressure-volume change test, shown in Fig. 3, indicate two different modes of behavior. When the suction is smaller than about 3 bars it appears that the soil samples

Table 1. Sample Data and Results of Suction-Pressure-Volume Change Tests

| Hole I.D. | CB-2 | CB-1 | CB-2 | CB-2 | CB-1 |
|---|---|---|---|---|---|
| Depth(m) | 0.45 | 0.7 | 1.1 | 1.6 | 2.4 |
| Initial Water Content($w_i$ : %) | 19.6 | 19.8 | 18.6 | 18.5 | 22.5 |
| Final Water Content($w_f$ : %) | 22.5 | 21.8 | 22.8 | 22.1 | 23.1 |
| Mean Confining Pressure($\sigma_c$ : kPa) | 14.0 | 19.0 | 38.0 | 48.9 | 76.6 |
| Dry unit Wt.($\gamma_d$ : g.cm3) | 1.60 | 1.60 | 1.62 | 1.69 | 1.57 |
| Initial Suction($\Psi_i$ : Bars) | 9.5 | 9.3 | 15.0 | 7.3 | 3.3 |
| Initial Suction($\Psi_f$ : Bars) | 2.0 | 2.2 | 1.5 | 1.5 | 2.0 |
| Volumetric Strain($\epsilon_v$ : %) | 4.8 | 4.7 | 4.0 | 2.6 | 0.23 |

no longer swell and that there is just a steady decrease in the soil suction. When soil suction is larger than about 3 bars, the $\epsilon_v - \Psi$ relationship for the soil is approximately linear on a strain-log suction scale, i.e.,

$$\epsilon_v(\%) = C_1 \log(\Psi) + C_2, \tag{9}$$

where $C_1$ and $C_2$ are constants.

The appropriate regression equations based on Eq. 9 are shown in Table 2.

The overall regression equation that relates $\sigma_c$ and $\Psi$ can be expressed as

$$\epsilon_v(\%) = (9.14 - 0.12\sigma_c)\ (1.28 - \log\Psi) \qquad (\Psi \geq 3\text{bars}) \tag{10}$$

Equation (10) is valid when $\sigma_c$ is less than 76 kPa.

### 3.4 Determination of $C_t$, $C_m$ and Constitutive Surface

Free swell tests were performed to obtain the compression index ($C_t$). In the free swell oedometer test, the specimen is allowed to swell under a pressure of 3 kPa by submerging the

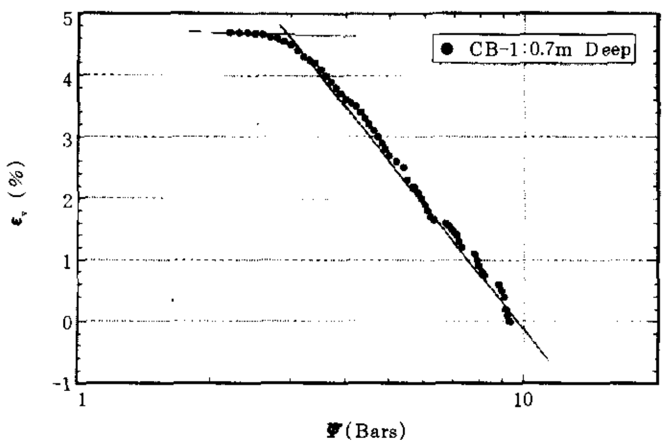


Fig.3 $\epsilon_v$ vs. suction($\Psi$) (CB-1:0.7m Deep)(1Bar=100kPa)

Table 2. Regression Relationships

| Hole I.D. | Depth (m) | $\sigma_c$(kPa) | Regression Equation |
|---|---|---|---|
| CB-2 | 0.45 | 14.0 | $\epsilon_v = 9.45 - 7.40\ \log(\Psi)$ |
| CB-1 | 0.7 | 19.0 | $\epsilon_v = 9.23 - 7.25\ \log(\Psi)$ |
| CB-2 | 1.1 | 38.0 | $\epsilon_v = 6.55 - 4.44\ \log(\Psi)$ |
| CB-2 | 1.6 | 48.9 | $\epsilon_v = 4.32 - 3.66\ \log(\Psi)$ |
| CB-1 | 2.4 | 76.6 | $\epsilon_v = 0.62 - 0.42\ \log(\Psi)$ |

Note : $\Psi$ is expressed in bars, $\epsilon_v$ is in %

specimen in the distilled water. After attaining an equilibrium condition, the soil specimen is then loaded following the conventional oedometer test procedure.

The slope of the loading curve plotted on a semi-logarithmic scale gives the compression index, 6.90 (Kim, 1996).

While determining the suction index ($C_m$), Lytton (1994) observed that the mean principal stress increases only slightly in the shallow zones where most of the volume change take place. Thus it is commonly sufficient to compute the final mean principal stress, $\sigma_{cf}$, from the overburden, surcharge, and foundation pressure and treat the initial mean principal pressure, $\sigma_{ci}$, as a constant corresponding to the stress-free suction vs. volumetric strain line represented by Eq. 1. Because there is no zero on a logarithmic scale, $\sigma_{ci}$ may be regarded as a material property, i.e., a stress level below which no correction for overburden pressure must be made in order to estimate the volumetric strain. It has been found to correspond to the mean principal stress at a depth of 40 cm. Thus, the slope in the regression equation of sample at the depth of 0.45m in suction-pressure-volume change test was used as the suction index of NGES-UH site (Table 2, CB-2, 0.45m), i.e., 7.40.

The three-dimensional constitutive surface for NGES-UH site according to Fredlund's method can be approximated as

$$d\varepsilon_v\ (\%) = 6.90\ \Delta\log\sigma_c + 7.40\ \Delta\log\Psi \qquad (11)$$

The three-dimensional constitutive surface for volume change is shown in Fig. 4.

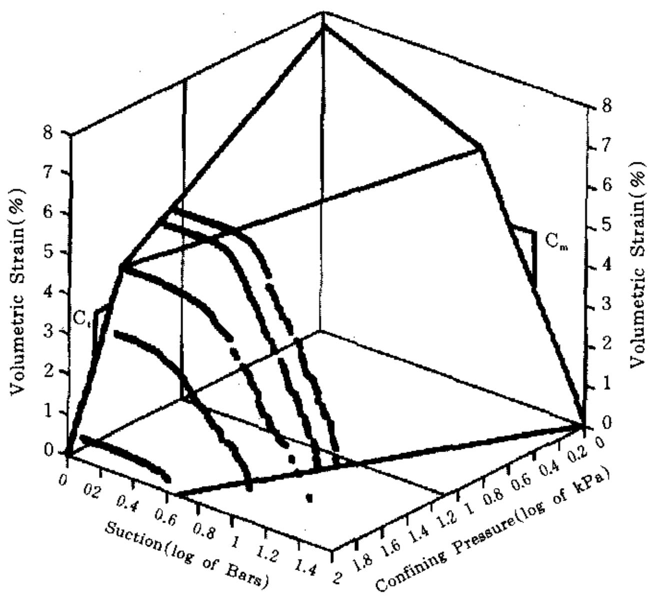


Fig.4 Three-Dimensional Suction-Pressure-Volumetric Strain Constitutive Surface for NGES-UH Site

## 4. Field Test

### 4.1 Test Site Layout and Installation of Instruments

Three isolation-tube shafts and one reference drilled shaft, 0.305m in diameter and 4.2m deep, were installed. Figures 5 and 6 show the test site layout, indicating locations of instruments and drilled shafts, and a section view showing dimensions of the drilled shafts and the locations of the ground instruments.

Two types of instruments were installed to measure suction. The instrument selected for installation was a device distributed by SOILTEST, Inc., that consisted of fiberglass fibers whose collective resistivity changed as their moisture content changed. The second type of instrument was a thermocouple psychrometer with a 400 mesh stainless steel protective tip manufactured by the J.R.D. Merrill Company.

The test site was instrumented with six columns of suction sensors. Three of them were installed between the reference drilled shaft, R-1 and isolation tube shaft, I-2, and the remaining three columns were placed between R-1 and isolation tube shaft, I-1. Each column had three suction measuring points, 0.45m, 1.1m, and 2.0m below grade.

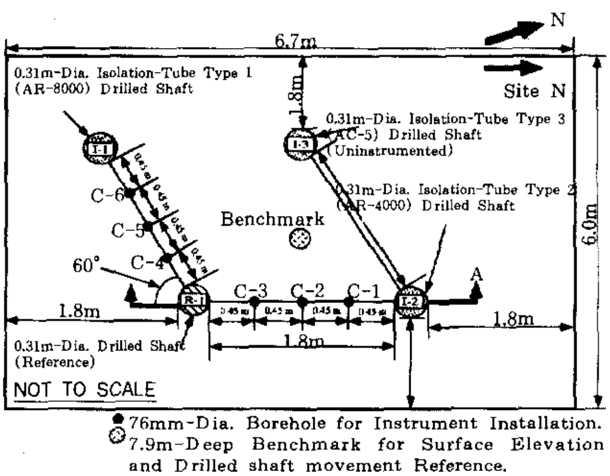


Fig.5 Plan View of Test Site Layout

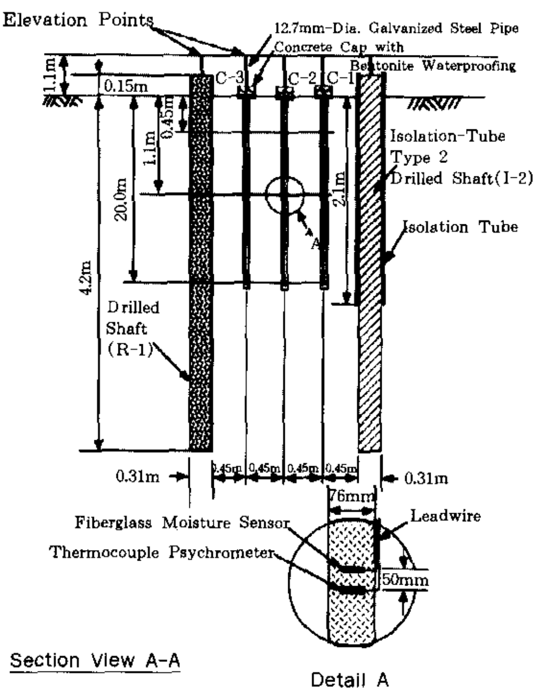


Fig.6 Section View Showing Dimensions of the Drilled Shafts and Locations of Ground Instruments

## 4.2 Isolation Tubes

Isolation tubes were also installed to a depth of 2.1m to bypass the potentially expansive surface soil unit. Asphalts with three different viscosities were provided in the isolation tubes. Isolation tube 1 (I-1) contained an AR-8000 grade asphalt, which was the most viscous of the three. Isolation tube 2 (I-2) contained AR-4000 grade asphalt, which was of intermediate viscosity, while Isolation tube 3 (I-3) contained AC-5 grade asphalt, which was the least viscous.

Figure 7 shows a schematic elevation of an isolation-tube drilled shaft.

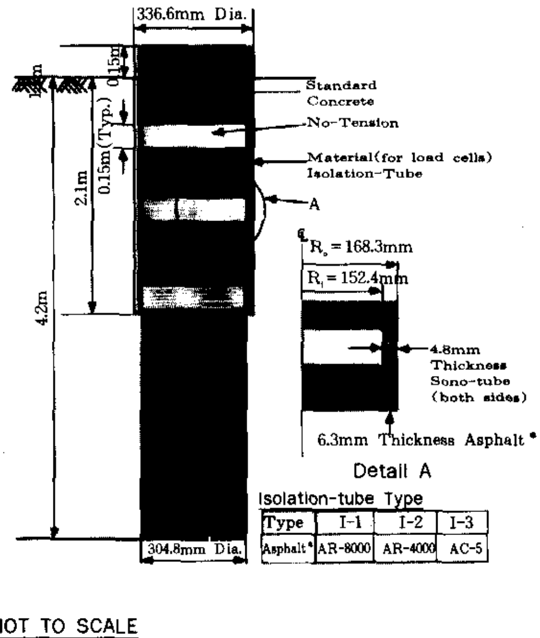


Fig.7 Isolation-tube Drilled Shafts

## 4.3 Elevation Measurements

A benchmark was established in the middle of research site. The benchmark was set at a depth of 7.9m, which is below the potential expansive zone and which can be considered stable. It served as the reference benchmark for the ground surface and shaft elevation measurements. The benchmark consisted of a 19mm diameter galvanized steel pipe supported on a 70mm diameter circular plate, the bottom which, in turn, rested on the bottom of a 102mm diameter augured borehole. The pipe was placed inside a 102mm diameter PVC pipe that had been driven approximately 25mm into the soil at the bottom of the borehole to seat it and seal off the inside from outside moisture intrusion. The benchmark pipe was supported laterally within the PVC pipe by loose fitting rings which maintained the pipe in an essentially vertical alignment. The PVC pipe was sealed internally with a bentonite slurry to ensure that no moisture from the surface could reach the soil at the bottom of the benchmark.

The test site had a total of six ground surface elevation and 4 drilled shaft elevation points. The elevation points for the ground surface elevation were constructed with 1m high ×12.7mm diameter galvanized steel pipes cast in concrete blocks 300mm×300mm×150mm high to hold the pipe in position. The elevation points for the drilled shafts, installed on the tops of shafts during curing, were 1m high×12.7mm diameter galvanized steel pipes. Elevation measurements were made at all the elevation points relative to the benchmark by using a manometer formed from 12.7mm I.D. clear plastic tubing. Elevations were read to the nearest 0.5mm. The difference in thermal elongation of the bench mark and elevation points was also considered because the exposed length of each was different. The difference in elongation was well within the precision of the manometer, which was 0.5mm.

### 4.4 Surface Elevation Changes

Elevation changes at six surface points are shown in Fig. 8. The surface elevation at the time of ground instrument installation was considered to be the reference elevation. The absolute elevation of the site was about +12.0m MSL. Maximum and minimum surface elevations changes at each measurement point are summarized in Table 3.

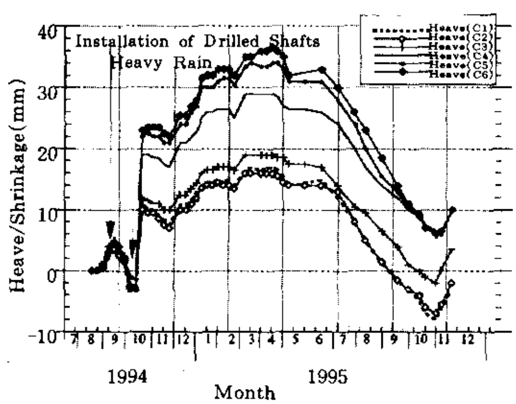


Fig. 8 Surface Elevation Change

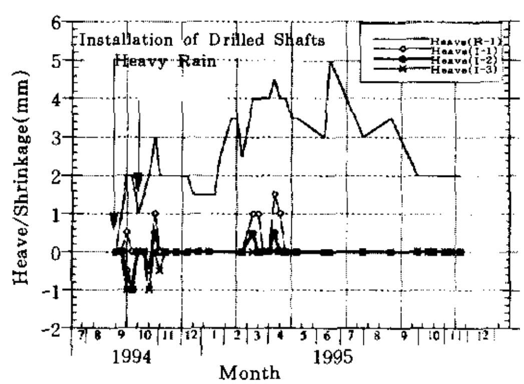


Fig. 9 Elevation Changes at the Head of Reference and Isolation-type Drilled Shafts

Table 3. Extreme Surface Elevations : July, 1994-November, 1995.

| Location | C1 | C2 | C3 | C4 | C6 | C6 |
|---|---|---|---|---|---|---|
| Max. elevation(mm) | +16 | +17 | +19 | +29 | +34 | +37 |
| Min. Elevation(mm) | -7 | −8 | −2 | −4 | −4 | −4 |
| Difference(mm) | 23 | 25 | 21 | 33 | 38 | 41 |

### 4.5 Shaft – Head Elevation Changes

September 2, 1994. The comparison of elevation changes between the heads of the reference drilled shaft and those of the isolation-tube shafts is shown in Fig. 9. The maximum upward vertical movement change of the reference drilled shaft was recorded at 5.0mm, while isolation tube shafts moved no more than 1.5mm (I-1). The shaft with the most viscous tube (I-1) recorded up to 1.5mm movement, and those with lower viscosity recorded 1.0mm upward movement.

Ratcheting of the outer tubes in the isolation tube arrangements occurred after the heavy rains of October 15 to 18, 1994. Ratcheting is defined as the permanent upward movement of the outer tube relative to the inner tube. The amount of ratcheting of the outer tubes was close to the surface elevation change two days after the heavy rain (25mm). It was lowest in the most viscous (I-1) tube and the tube of intermediate viscosity (I-2) and highest in the least viscous (I-3) tube.

### 4.6 Suction and Surface Elevation Changes

The typical suction and surface elevation are plotted as functions of time in Fig. 10.

Psychrometers provided quite reliable data during the first three months after installation before heavy rains. During this period, suction at depths of 0.45m and 1.1m showed similar high trends, ranging from 12.0 to 21.5 bars, and the change of surface elevation lagged behind the suction changes by 3 to 4 weeks. After the heavy rain of October, 1994, the surface elevation increased rapidly, ranging from 10mm (C1) to 23mm (C6), and measured suction decreased from about 5 bars to 1.5 – 2.0 bars in 5 weeks (the end of November, 1994).

During the wet and cool season (November, 1994 to March, 1995), surface elevation movement exhibited a different response with respect to suction changes. Suction values returned to around 5

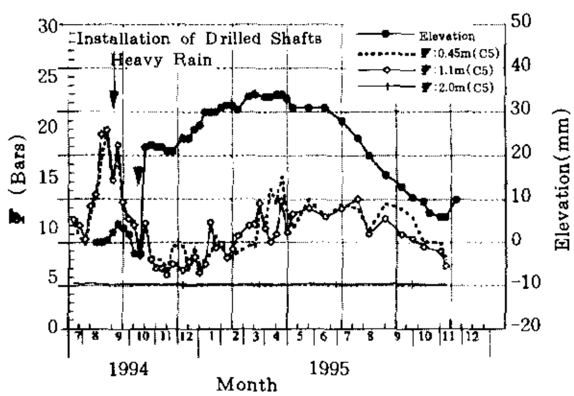


Fig. 10 Ψ vs. Surface Elevation(C5)(1Bar = 100kPa)

bars at the depth of 0.45m and 6 bars at the depth of 1.1m. Despite the trend of increasing suction values at depths of 0.45m and 1.1m, surface elevation continued increasing.

Suction increased to 10 bars on the north side by March, 1995 while on the south side it increased to 10 bars in April, 1995. Surface elevation was essentially constant during March and April, 1995, but began to decrease by the end of April. During the next five months (May to September) suction remained at around 10 bars on the south side and 8 bars on the north side. The surface elevation continued to decrease slightly until the end of October. Suction began to increase again at the end of October, 1995.

## 5. MODEL FOR HEAVE PREDICTION

### 5.1 Determination of the Active Zone Depth

The determination of the active zone depth ($z_a$) may be accomplished by several means, including long-term soil suction measurements, establishment of depth of ancient surface cracks, and establishment of depth of grass root zones (O'Neill, 1988). Suction measurements during the test period showed that the variation of suction values was quite wide at the depths of 0.45m and 1.1 m but almost negligible at the depth of 2.0m. This means that $1.1\text{m} < z_a < 2.0\text{m}$. Other methods involve determining the relationships of liquidity index to depth or water content/plastic limit to depth over several seasons. Envelopes to the relationships tend to become constant with depth below $z_a$. O'Neill (1988) showed that a typical depth of the active zone for the Beaumont formation on the University of Houston campus was 1.68m. Since this depth is located between 1.1m and 2.0m, it is reasonable to establish the active zone depth as 1.68m.

### 5.2 Determination of Suction Profiles for the NGES-UH

Soil suction theory can be used to establish a profile of limits within which the vertical soil suction profile will vary as the soil becomes drier during dry seasons or becomes wetter during periods of atmospheric wetness. This theory is applicable to conditions of static equilibrium; i.e., all variables affecting the state of soil suction equilibrium remain constant except the condition that affects the moisture flux. The moisture flux varies between two extremes: the driest and wettest conditions expected to occur during the period of interest. Thus, any climate-related conditions to which the site may be subjected over this period would produce profiles of suction that range between two extremes of wetness and dryness.

### 5.3 Equilibrium Suction Value ($\Psi_e$) and Limit Suction Value ($\Psi_o$) for the NGES-UH

The index properties were averaged down to the depth of 1.8m, approximately equal to the active zone depth, to estimate $\Psi_e$ and $\Psi_o$ for the NGES-UH (Kim, 1996). $\Psi_e = 3.5\text{pF}$ (3.0 bars) and $\Psi_o = 1.8\text{pF}$ are obtained for the NGES-UH. Limiting suction profiles from this method are shown in Fig. 11.

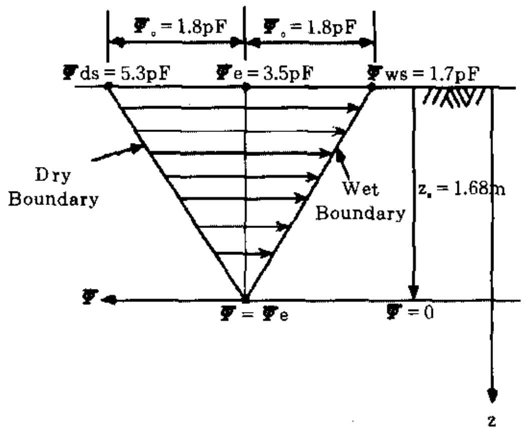


Fig. 11 Computed Boundary Soil Suction Profiles for the NGES-UH

### 5.4 Field Measurement and Boundary Suction Profile

To ascertain how closely the boundary suction profiles match the field measurements, eighteen months of field suction measurements are superimposed on the boundary suction profiles. To represent the most reasonable suction value to plot for each month, the weekly suction values were averaged at each depth in the six different columns, and among these averaged values, the highest value within the month was selected in the dry and hot periods and the lowest was selected in the wet and cool periods.

Suction values measured at the depth of 2.0m by using the fiberglass moisture sensors were very low (less than 0.3 bars) compared with the Mitchell equilibrium suction value (3.0 bars). This difference may come from reading error (the ideal reading range of fiberglass moisture sensors is 0 – 2.5 bars) or installation error [fiberglass moisture sensors are required to be situated in very intimate contact the surrounding soil (Lee and Wray, 1992), which may not have been completely achieved while installing the sensors in the field.]. Thus, it is more reasonable to use 3.0 bars as the equilibrium suction values at the depth of 1.68m for the purpose of computing surface movements and uplift stresses in the shafts. The measured suction values fall within the boundary suction profiles except for 2 points measured at the depth of 1.1m in August and September, 1994, which are only slightly outside of the computed dry envelope (Kim, 1996).

### 5.5 Heave Prediction

The main components of heave prediction are the initial soil suction profile, the final soil suction profile, the suction or compressibility index parameter, and the depth of the active zone.

The highest suction values were measured in September 1994, which occurred within a few days after shaft installation. The suction profile at this time was selected as the initial suction profile.

For the purpose of this study, two trial profiles were selected for the final suction profile: (1) the lowest soil suction profile based on field measurements and (2) the wet boundary.

The suction indexes were calculated from Eq 10 with different confining pressures, corresponding with different soil depths. The initial and final suction profiles are shown in Fig. 12. The surface heave prediction calculations are summarized in Table 4.

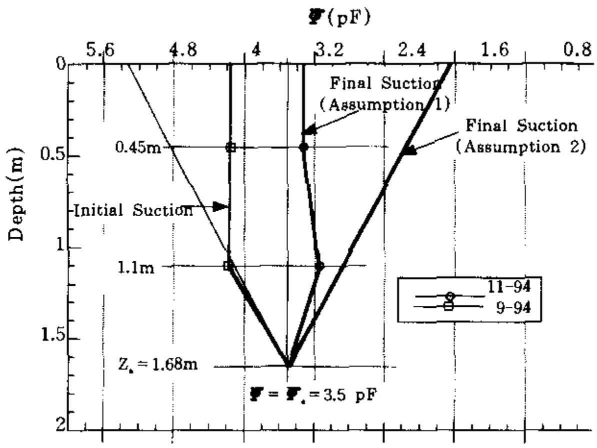


Fig. 12 Design Suction Profile for Heave Prediction

Table 4. Calculation of Hgeave

| Depth (mm) | Layer Thicknes s (mm) | Confining Pressure, $\sigma_c$ (kPa) | Compressi -bility Index[1] $C_\Psi$ | Initial Suction, $\Psi_i$ (Bar) | Final Suction, $\Psi_f$ (Bar) | | Heave Prediction (mm) | |
|---|---|---|---|---|---|---|---|---|
| | | | | | Assump.1 | Assump.2 | Assump.1 | Assump.2 |
| 0~450 | 450 | 12.3 | 0.077 | 14.2 | 2.1 | 0.8 | 28.7 | 77.9 |
| 450~750 | 300 | 24.5 | 0.062 | 14.4 | 1.9 | 0.2 | 16.3 | 53.11 |
| 750~1100 | 350 | 37.2 | 0.047 | 15.2 | 1.6 | 0.5 | 16.1 | 40.8 |
| 1100~1680 | 580 | 52.4 | 0.029 | 5.5 | 2.2 | 1.5 | 6.7 | 9.5 |
| [1] from Eq 10 | | | | | | Total Have (mm) | 67.9 | 181.4 |

In case of assumption 1 for the wet profile, the amount of total heave was calculated to be 67.9mm. An empirical cracking factor ($\xi$) should be considered for estimating the actual heaving amount. The maximum measured surface elevation changes, as shown in Table 6, ranged from 21mm to 41mm. Thus the empirical cracking factor ($\xi$) can be obtained as 0.3 to 0.6 for the NGES – UH. For assumption 2, the total calculated surface heave was 181.4mm. Using $\xi = 0.45$ (average of 0.3 and 0.6), it appears possible that 81mm of heave ($0.45 \times 181.4$mm) could have occurred if the site had been fully soaked for a long period of time.

## 6. Conclusions

A computational model based on suction concept was developed to predict the maximum ground movement. Furthermore, a simple technique (isolation tube) was investigated to mitigate the negative seasonal movements of expansive soils on the performance of drilled shafts. The followings are conclusions of the study.

Rapid changes in vertical movement in the soil occurred to a depth of approximately 1.0m with the application of saturating moisture (heavy rain). Maximum ground movements exceeding 35mm were observed during the life of the experiment. Movements of only 1 to 2mm were observed in the test shafts with isolation tubes, while 4 to 5mm were observed in the reference shaft. The ground movements were computed from suction changes with an empirical cracking factor ($\xi$) of 0.3 – 0.6, with a most probable value of 0.45.


## Acknowledgements

This work was supported by Grant from Inje University. Dr. Warren K. Wray and Mr. Edward H. Lee of Texas Tech University graciously assisted in the calibration of the suction instruments.


## References


1. Aitchison, G.D., and Martin, R. (1973), "A Membrane Oedometer for Complex Stress – Path Studies in Expansive Clays," *Proceedings, 3rd International Conference on Expansive Soil*, Haifa, Israel, Vol. 2, pp. 83 – 88.
2. Brackley, I.J.A. (1971), "Partial Collapse in Unsaturated Expansive Clay," *Proceedings, 5th Reg. Conference on Soil Mechanics and Foundation Engineering*, South Africa, pp. 23 – 30.
3. Fredlund, D.G. (1983), "Prediction of Ground Movements in Swelling Clays," Presented at the 31st Annual Soil Mechanics & Foundation Engineering Conference, ASCE, Invited Lecture, Minneapolis, MN.
4. Fredlund, D.G., and Morgenstern, N. R. (1976), "Constitutive Relations for Volume Change in Unsaturated Soils," *Canadian Geotechnical Journal*, Vol. 13, No. 3, pp. 261 – 276.
5. Johnson, L.D., and Snethen, D.R. (1978), "Prediction of Potential Heave of Swelling Soils," *Geotechnical Testing Journal*, ASTM, Vol. 1, No. 3, pp. 117 – 124.
6. Kim, M. H. (1996), "Effect of an Expansive Clay on the Behavior of Drilled Shaft," Ph. D. Dissertation, University of Houston, Houston TX.
7. Lee, H.C., and Wray, W.K. (1992), "Evaluation of Soil Suction Instruments," *Proceedings, 7th International Conference on Expansive Soil*, Dallas, TX, Vol. 1, pp. 307 – 312.
8. Lytton, R.L. (1994), "Prediction of Movement in Expansive Clays," *ASCE Geotechnical Special Publication*, No. 40, pp. 1827 – 1845.
9. McKeen, R.G. (1992), "A Model for *Predicting Expansive Soil Behavior*," *Proceedings, 7th International Conference on Expansive Soils*, Dallas, TX, Vol. 1, pp. 1 – 6.
10. O' Neill, M.W. (1988), "Adaptive Model for Drilled Shafts in Expansive Clay," *ASCE Geotechnical*

*Special Publication*, No. 16, pp. 1 – 20.

11. O'Neill, M.W., and Poormoayed, N. (1980), "Methodology for Foundations on Expansive Clays," *Journal of the Geotechnical Engineering Division*, ASCE, Vol. 106, No. GT 12, December, pp. 1465 – 1488.
12. O'Neill, M.W., and Yoon, G. (1995), "Some Engineering Properties of Overconsolidated Pleistocene Soils of the Texas Gulf Coast," *Transportation Research Record*, No. 1479, pp. 81 – 88.
13. Wiggins, J.H., Slossen, F.E., and Krohn, J.P. (1978), Natural Hazards: *Earthquake, Landslide, Expansive Soil*, J.H. Wiggins Co., Report prepared for the NSF, Grant No. ERP – 75 – 09998 and No. AEN – 74 – 23993.

(접수일자 1998. 5. 30)